

Parametric Studies of Directed Fragmentation Warhead Used for Combat Shaped Charges

Robert PANOWICZ, Jacek NOWAK,
Marcin KONARZEWSKI, Tadeusz NIEZGODA

*Military Technical Academy, Faculty of Mechanical Engineering
Department of Mechanics and Applied Computer Science
Kaliskiego 2, 00-908 Warszawa, Poland
e-mail: {rpanowicz, jnowak, mkonarzewski, tniezgoda}@wat.edu.pl*

The aim of this paper is to present the results of research on the influence of fragmentation liner material parameter on spreading capabilities. A fragmentation liner is a part of a directed fragmentation warhead used to combat shaped charges and consisting of metal balls embedded in the resin. In addition, the case of the fragmentation warhead and the surrounding air were also modeled. Four variants of numerical analyses were prepared, differing in the value of maximum plastic strain characterizing the fragmentation liner. C-4 explosive was used for driving the liner fragmentation. In order to properly describe the behaviour of the fragmentation warhead, Arbitrary-Lagrangian Eulerian (ALE) and Fluid-Structure Interaction (FSI) approach was used. A three dimensional model of directed fragmentation warhead along with the fragmentation liner was prepared in MSC Patran software and numerical analyses were performed using LS-Dyna software. As a result of numerical analyses, the maximum velocity and a spreading angle in both the vertical and horizontal plane of the fragmentation liner were determined in each case.

Key words: finite elements method, dynamic, directed fragmentation warheads.

1. INTRODUCTION

The growing threat to military vehicles from shaped charges enforces development of solutions to improve protection against this type of threat. A shaped charge is a kind of projectile which uses a cumulative stream to pierce the armor. This stream is created by the detonation of an explosive charge and its impact on the metal liner having most often a conical shape. One of the most commonly used shaped charge is PG-7 missile (Fig. 1).

So far, the most common solutions have been passive protection systems in the form of nets and bar armors. Currently, the active defense systems against

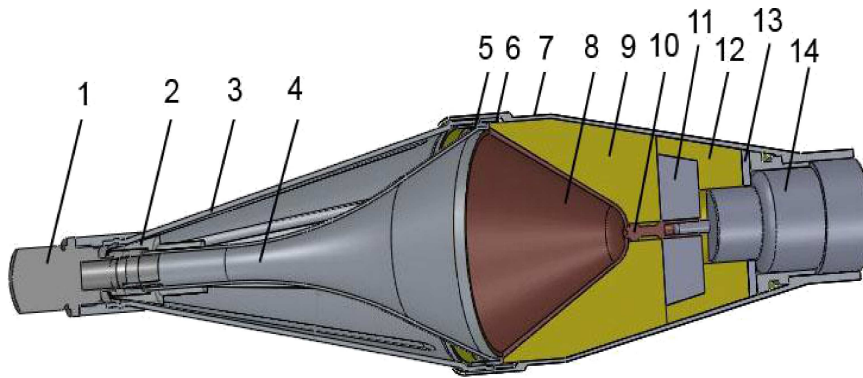


FIG. 1. PG-7G warhead cross-section: 1) warhead cap, 2) head part of the igniter, 3) ballistic cap, 4) conductive cone, 5) insulating ring, 6) isolator, 7) warhead case, 8) liner, 9) explosive charge, 10) conductor, 11) shutter, 12) explosive charge, 13) roller, 14) bottom part of the igniter.

shaped charges become more and more popular. Two main groups can be distinguished among the active defense systems:

- softkill systems – their purpose is to influence the electronic systems of an approaching missile,
- hard-kill systems – their purpose is to physically damage or destroy the approaching threat; typically, they destroy the structure of the missile or interfere with initiation of the cumulative stream by damaging the fragmentation liner.

A directed fragmentation warhead is one of such hard-kill systems.

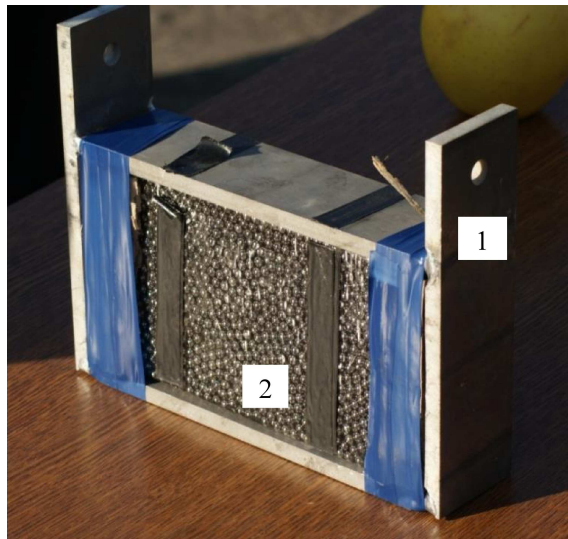


FIG. 2. Directed fragmentation warhead: 1) case, 2) fragmentation liner.

Such a warhead consists of a metal case (1) along with an explosive charge and a fragmentation liner (2). For an optimal angle of fragments dispersion and their energy, the appropriate selection of an explosive charge and fragmentation liner parameters is necessary.

Numerical analyses were performed using ALE and FSI approach. In this method, the fragmentation liner is modeled using Lagrange description while the resin, the explosive charge and the surrounding air are modeled using Euler description.

2. THE MODEL OF DIRECTED FRAGMENTATION WARHEAD

The model of a directed fragmentation warhead consists of four main parts: the metal case, the explosive charge, the fragmentation liner (metal balls embedded in resin) and the surrounding air. Due to the fact that the analysed phenomenon is symmetrical, only a half of the system was modeled. This allowed for significant reduction of the finite elements in the model and reduced the time required to carry out the numerical analyses.

The fragmentation liner (Fig. 3) consists of 1620 balls (5.5 mm in diameter) embedded in the resin. For their description, 74 520 solid finite elements were used. A description of material parameters was prepared in four variants: one case corresponding to the rigid material and three cases of deformable material corresponding to various heat treatments (variation considering the applied value of maximum plastic strain at failure). To describe the elements as non-deformable, RIGID type material was used. In the case of deformable balls,

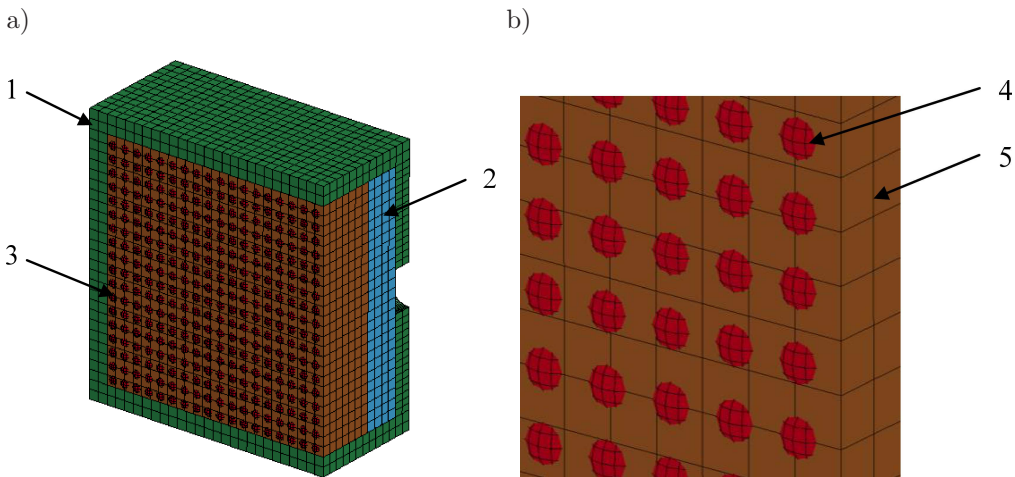


FIG. 3. Numerical model of directed fragmentation warhead: 1) metal case, 2) explosive charge, 3) fragmentation liner, 4) balls, 5) resin.

a bilinear material model with parameters corresponding to the S350 (St3 in the old classification) steel was used. In this constitutive model material behaviour is described by three characteristic points determining the stress and strain at which it occurs (ES, EPS). It is assumed that the starting point corresponds to zero strain. Material behaviour is linear between points. Material constants used in numerical analyses are presented in Table 1.

Table 1. Material parameters for the balls.

Parameter	Description	Units	Value
ρ	density	kg/m ³	7890
E	Young's modulus	GPa	210
ν	Poisson's ratio	–	0.3
ε_f	plastic strain to failure	–	0.2; 0.4; 0.7
EPS1	first effective plastic strain value	–	0.02
EPS2	second effective plastic strain value	–	0.4
ES1	corresponding yield stress value to EPS1	GPa	0.21
ES2	corresponding yield stress value to EPS2	GPa	0.218

Mechanical properties of the case made of S350 steel were described using a simplified Johnson-Cook type material [1]. This model correctly reproduces the behaviour of the described material during dynamic interaction with high strain rates and strains but does not include the thermal effects. Johnson-Cook model allows for the specification of a yield point stress limit by a linear relationship in a logarithmic scale of strain rate [2]:

$$\sigma_{\text{flow}} = [A + B(\varepsilon^p)^n] \left(1 + C \ln \dot{\varepsilon}^{p*}\right),$$

where A, B, C, n – material constants $\dot{\varepsilon}^{p*} = \dot{\varepsilon}^p / \dot{\varepsilon}_0^p$ – normalized effective plastic strain rate, $\dot{\varepsilon}^{p*}$ – effective plastic strain rate, $\dot{\varepsilon}_0^p$ – quasi-static threshold strain rate.

Parameters used in simulation taken from the literature [1] are shown in Table 2.

For driving the fragmentation liner, a commonly used C-4 explosive was chosen. Initially, for this purpose, TNT explosive was considered. Unfortunately it has worse propellant parameters such as Gurney's velocity. This translates into much smaller velocity of fragmentation liner, as observed during numerical analyses carried out in the previous work of authors [2].

Table 2. Material parameters for the case [1].

Parameter	Description	Units	Value
ρ	density	kg/m ³	7890
E	Young's modulus	GPa	210
ν	Poisson's ratio	–	0.3
A	material constant	GPa	0.365
B	material constant	GPa	0.51
n	material constant	–	0.9
C	material constant	–	0.0936
ε_f	plastic strain to failure	–	0.3

The detonation process was described using programmed burn model approximations [3, 4], and the behaviour of the detonation products was described with the JWL (John, Wilkins, Lee) equation [1, 5]:

$$p = A \left(1 - \frac{\omega}{R_1 V} \right)^{-R_1 V} + B \left(1 - \frac{\omega}{R_2 V} \right)^{-R_2 V} + \omega \rho E,$$

where $V = \rho_0/\rho$, ρ_0 – initial density, ρ – density of detonation products, A , B , R_1 , R_2 , ω – constant values.

The surrounding air was described using Mie-Gruneisen equation [3, 4]:

$$p = p_0 + \gamma \rho E,$$

where p – pressure, p_0 – initial pressure, γ – Gruneisen coefficient, ρ – density, E – specific internal energy. Due to the fact that resin has low strength compared to other materials, the same material model was used for its description.

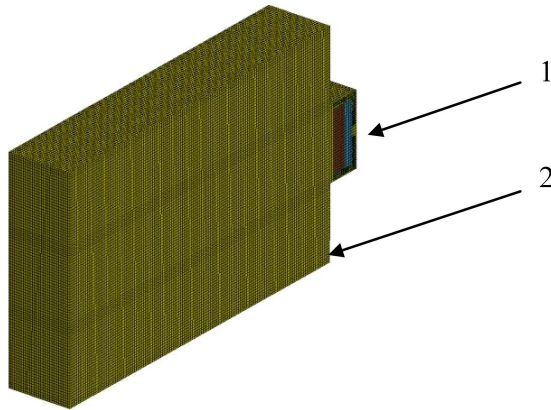


FIG. 4. Directed fragmentation warhead model with air:
1 – directed fragmentation warhead, 2 – air.

The following constant values in the equation were taken from the literature [6]: $\gamma = 1.4$, $\rho = 1.185 \text{ kg/m}^3$, $p_0 = 1013 \text{ hPa}$.

3. NUMERICAL ANALYSES

On the boundaries of Eulerian domain (air) non-reflecting conditions were assumed, while between all the elements described by Lagrange equations defined surface-to-surface contact type.

The analysis of the phenomenon begins at the moment $t = 0$ in which the process of detonation starts.

Numerical analyses were carried in four variants of material from which fragmentation liner is constructed:

- 1) rigid material,
- 2) bilinear material with $\varepsilon_f = 0.2$,
- 3) bilinear material with $\varepsilon_f = 0.4$,
- 4) bilinear material with $\varepsilon_f = 0.7$,

where ε_f is maximal plastic strain at which the element is destroyed.

For such selected materials, the velocity reached by the balls has been studied (Figs. 6–9). Velocity was determined for five balls located closest to the center of the destructor in separated layers (Fig. 5). In addition, the behaviour of the balls during the detonation and the angle of their spread (in both the vertical



FIG. 5. Location of studied balls.

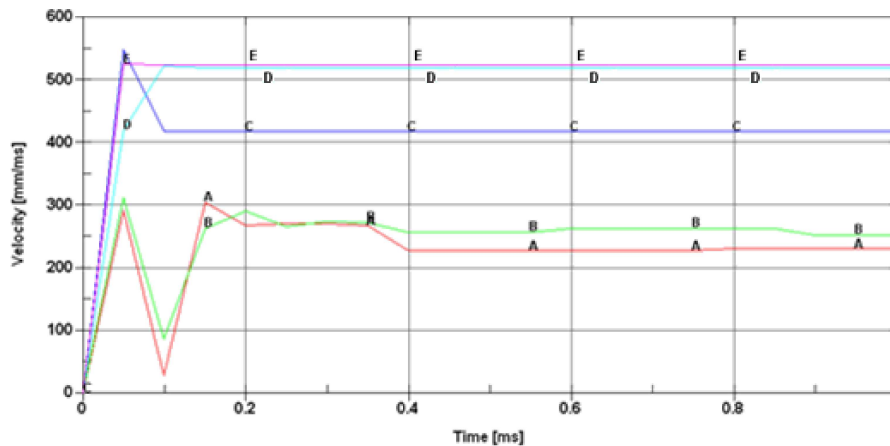


FIG. 6. Balls velocity, rigid material, A, B, C, D, E – studied balls.

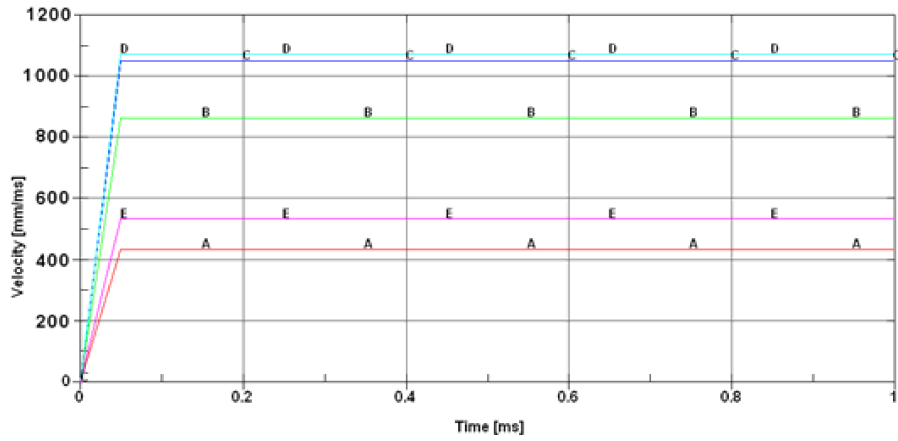


FIG. 7. Balls velocity, bilinear material $\varepsilon_f = 0.2$, A, B, C, D, E – studied balls.

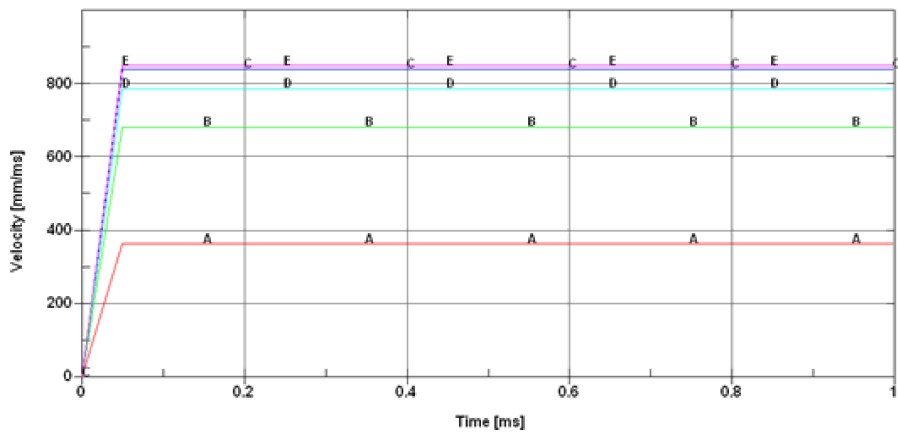


FIG. 8. Balls velocity, bilinear material $\varepsilon_f = 0.4$, A, B, C, D, E – studied balls.

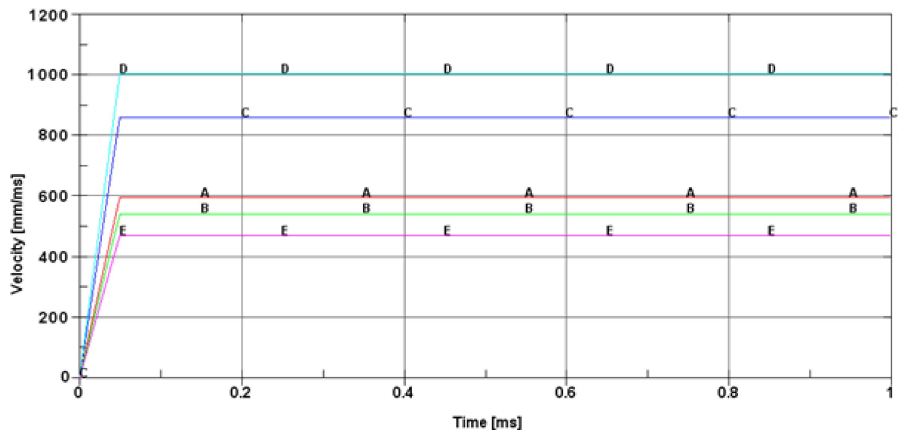


FIG. 9. Balls velocity, bilinear material $\varepsilon_f = 0.7$, A, B, C, D, E – studied balls.

and horizontal plane) have been studied (Figs. 10–12). The results are shown for the selected moments in time.

The lowest value of velocity for bilinear material was obtained for balls with $\varepsilon_f = 0.4$ and was about 20% lower than in the case of $\varepsilon_f = 0.2$ and $\varepsilon_f = 0.7$. The angle of balls dispersion (Figs. 9–11) remained at similar level of about 110° in the horizontal plane and 105° in the vertical plane.

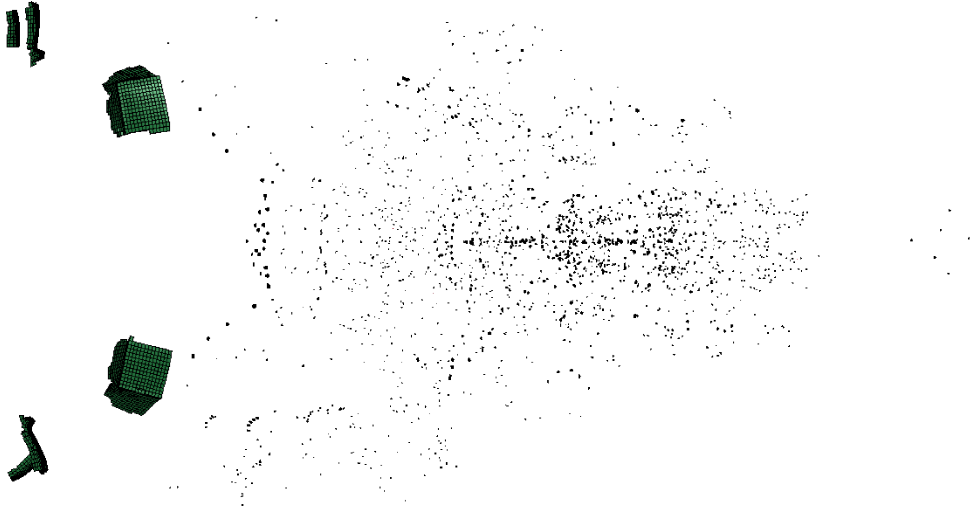


FIG. 10. The angle of balls dispersion in vertical plane – bilinear material $\varepsilon_f = 0.2$.

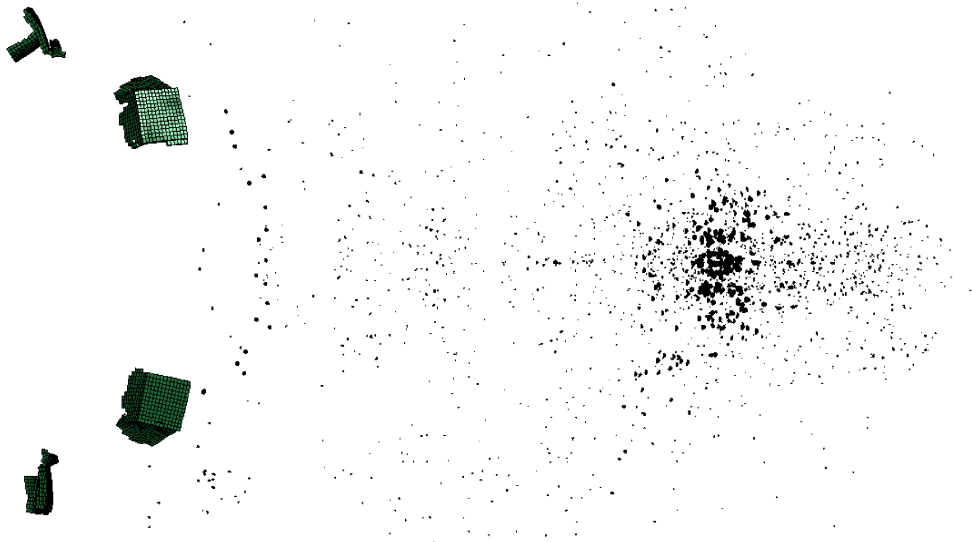


FIG. 11. The angle of balls dispersion in vertical plane – bilinear material $\varepsilon_f = 0.4$.

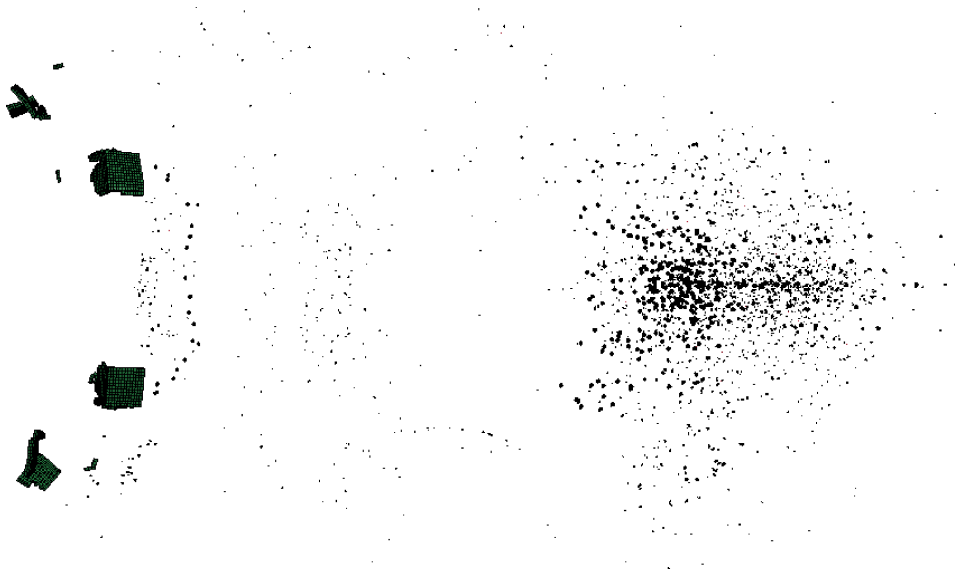


FIG. 12. The angle of balls dispersion in vertical plane – bilinear material $\varepsilon_f = 0.7$.

The collective results are shown in Table 3.

Table 3. Results of numerical analyses.

Material	Maximum velocity [m/s]	Angle of dispersion: horizontal plane	Angle of dispersion: vertical plane
rigid	550	114°	104°
$\varepsilon_f = 0.2$	1080	109°	104°
$\varepsilon_f = 0.4$	870	118°	106°
$\varepsilon_f = 0.7$	1005	110°	108°

4. SUMMARY

On the basis of the performed numerical analyses, the following conclusions can be drawn:

1. In order to properly describe the behaviour of the fragmentation warhead, ALE and FSI approach is strongly recommended,
2. The use of rigid elements results in obtaining the accurate values of the angles of dispersion, close to the values obtained in the case of bilinear material,
3. In the case of maximum velocity, there can be observed a clear difference between the results obtained for the bilinear material and for the rigid material.

REFERENCES

1. BDZIL J.B., STEWART D.S., JACKSON T.L., *Program burn algorithms based on detonation shock dynamics: discrete approximations of detonation flows with discontinuous front models*, J. Comput. Phys., **174**, 870–902, 2001.
2. PANOWICZ R., NOWAK J., KONARZEWSKI M., NIEZGODA T., *Introduction to numerical analysis of directed fragmentation warheads*, Journal of KONES Powertrain and Transport, **20**, 4, 2013.
3. HALLQUIST J.O., *Ls-Dyna theory manual*, Livermore Software Technology Corporation, Livermore, 2005.
4. JACH K. [Eds.], *Computer modeling of the dynamic interaction of bodies using the free points method*, [in Polish: *Komputerowe modelowanie dynamicznych oddziaływań metodą punktów swobodnych*], PWN, Warszawa, 2001.
5. KAPILA A.K., BDZIL J.B., STEWART D.S., *On the structure and accuracy of programmed burn*, Combustion Theory and Modelling, **10**, 2, 2006.

Received July 9, 2014; accepted December 10, 2014.
